

AD-A164 494

CHARACTERIZATION OF ALUMINUM NITRIDE/ALUMINUM OXIDE  
REACTIVELY SPUTTERED (U) NAVAL WEAPONS CENTER CHINA  
LAKE CA L KOSHIGOE ET AL SEP 85 NMC-TP-6651

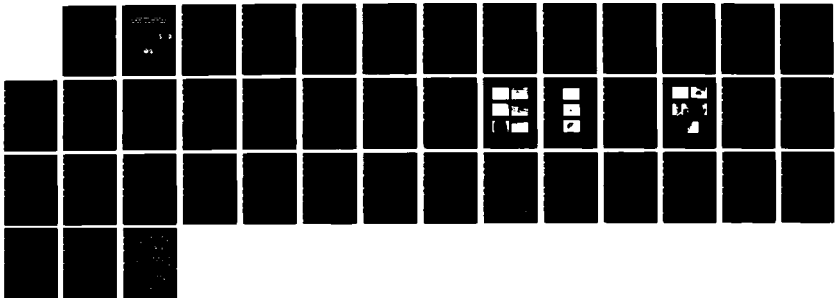
1/1

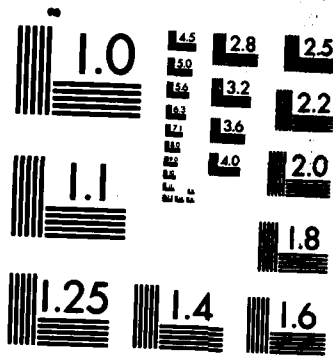
UNCLASSIFIED

SBI-AD-E900 539

F/G 20/5

NL





MICROCOPY RESOLUTION TEST CHART  
NATIONAL BUREAU OF STANDARDS-1963-A

E900539

12

NWC TP 8651

AD-A164 494

# Characterization of Aluminum Nitride/Aluminum Oxide Reactively Sputtered Antireflection Coatings

by  
L. G. Koshigoe  
*Engineering Department*

and  
L. F. Johnson  
T. M. Donovan  
C. D. Marrs  
*Research Department*

SEPTEMBER 1985

DTIC  
SELECTE  
FEB 19 1986  
S D

NAVAL WEAPONS CENTER  
CHINA LAKE, CA 93555-6001



Approved for public release;  
distribution is unlimited.

DTIC FILE COPY

86 2 18 245

# Naval Weapons Center

## FOREWORD

The work described in this report was performed by the Naval Weapons Center, China Lake, Calif., under Arpa Order 3343. This report is a preliminary study of the multilayer system  $AlN/Al_2O_3$  and its resistance to certain environmental conditions. The work described was carried out during FY 1984.

The report has been reviewed for technical accuracy by A. D. Baer and J. L. Stanford.

Approved by  
D. J. RUSSELL, Head  
Engineering Department  
24 September 1985

Under Authority of  
K. A. DICKERSON  
Capt., U.S. Navy  
Commander

Released for publication by  
B. W. HAYS  
Technical Director

NWC Technical Publication 6651

Published by.....Engineering Department  
Collation.....Cover, 19 leaves  
First Printing.....250 unnumbered copies

REPORT DOCUMENTATION PAGE

|   |   |  |                                  |
|---|---|--|----------------------------------|
| 1a REPORT SECURITY CLASSIFICATION<br><b>UNCLASSIFIED</b>  |   | 1b RESTRICTIVE MARKINGS  |                                  |
| 2a SECURITY CLASSIFICATION AUTHORITY  |   | 3 DISTRIBUTION/AVAILABILITY OF REPORT<br><b>A Statement</b>  |                                  |
| 2b DECLASSIFICATION/DOWNGRADING SCHEDULE  |   |  |                                  |
| 4 PERFORMING ORGANIZATION REPORT NUMBER(S)<br><b>NWC TP 6651</b>  |   | 5 MONITORING ORGANIZATION REPORT NUMBER(S)   |                                  |
| 6a NAME OF PERFORMING ORGANIZATION<br><b>Naval Weapons Center</b>   | 6b OFFICE SYMBOL<br><i>(if applicable)</i>          | 7a NAME OF MONITORING ORGANIZATION   |                                  |
| 6c ADDRESS (City, State, and ZIP Code)<br><b>China Lake, CA 93555-6001</b>  |   | 7b ADDRESS (City, State, and ZIP Code)   |                                  |
| 8a NAME OF FUNDING/SPONSORING ORGANIZATION<br><b>Naval Weapons Center</b>   | 8b OFFICE SYMBOL<br><i>(if applicable)</i>          | 9 PROCUREMENT INSTRUMENT IDENTIFICATION NUMBER   |                                  |
| 8c ADDRESS (City, State, and ZIP Code)<br><b>China Lake, CA 93555-6001</b>  |   | 10 SOURCE OF FUNDING NUMBERS   |                                  |
|   |   | PROGRAM ELEMENT NO.  | TASK NO. <b>Arpa Order 3343</b>  |
| 11 TITLE (Include Security Classification)<br><b>CHARACTERIZATION OF ALUMINUM NITRIDE/ALUMINUM OXIDE REACTIVELY SPUTTERED ANTIREFLECTION COATINGS (U)</b>   |   |  |                                  |
| 12 PERSONAL AUTHOR(S)<br><b>Koshigoe, L. G.; Johnson, L. F.; Donovan, T. M.; Marrs, C. D.</b>   |   |  |                                  |
| 13a TYPE OF REPORT<br><b>Final</b>  | 13b TIME COVERED<br>FROM <b>1984</b> TO <b>1984</b> | 14 DATE OF REPORT (Year, Month, Day)<br><b>1985, September</b>   | 15 PAGE COUNT<br><b>36</b>       |
| 16 SUPPLEMENTARY NOTATION   |   |  |                                  |
| 17 COSATI CODES   |   | 18 SUBJECT TERMS (Continue on reverse if necessary and identify by block number)   |                                  |
| FIELD   | GROUP   | SUB-GROUP  |                                  |
|   |   | <b>AlN/Al<sub>2</sub>O<sub>3</sub> Multilayer, Antireflection Coatings, Electron Beam Irradiation, Fluorine Exposure, Humidity, Laser Damage</b> |                                  |
| 19 ABSTRACT (Continue on reverse if necessary and identify by block number)   |   |  |                                  |
| <p>(U) Aluminum nitride/aluminum oxide multilayer protective antireflection coatings are being developed for use on laser windows. These materials have been shown to be relatively stable and scratch resistant, thus demonstrating their applicability for this use. Both two- and three-layer coatings were designed at the wavelength of 0.500<math>\mu</math>m. The design techniques utilized, as well as the resulting transmission spectra, are discussed. Single-layer films have been deposited on fused quartz and calcium fluoride substrates, and a three-layer film has been deposited on a fused quartz substrate. Studies of the resistance of these films to various environmental conditions including laser radiation, fluorine, electron beam irradiation, and humidity are presented. Surface analysis techniques such as scanning Auger microscopy (SAM), scanning electron microscopy (SEM), energy dispersive X-ray microanalysis (EDX), X-ray photoelectron spectroscopy (XPS), and Nomarski microscopy were used to examine coating composition and stoichiometry. Preliminary measurements on the laser resistance of the materials indicate that damage at defects is the predominant failure mode.</p> |   |  |                                  |
| 20 DISTRIBUTION/AVAILABILITY OF ABSTRACT<br><input type="checkbox"/> UNCLASSIFIED/UNLIMITED <input type="checkbox"/> SAME AS RPT <input checked="" type="checkbox"/> DTIC USERS   |   | 21 ABSTRACT SECURITY CLASSIFICATION<br><b>Unclassified</b>   |                                  |
| 22a NAME OF RESPONSIBLE INDIVIDUAL<br><b>Leslie G. Koshigoe</b>   |   | 22b TELEPHONE (Include Area Code)<br><b>(619) 939-3364</b>   | 22c OFFICE SYMBOL<br><b>3941</b> |

**UNCLASSIFIED**

**SECURITY CLASSIFICATION OF THIS PAGE**

**UNCLASSIFIED**

**SECURITY CLASSIFICATION OF THIS PAGE**

CONTENTS

Introduction..... 3

Multilayer Designs..... 4  
 Two-Layer Design..... 4  
 Three-Layer Design..... 7

Sample Preparation.....11

Film Structure.....16

Results.....19  
 Laser Radiation.....19  
 Fluorine Exposure.....24  
 Electron Beam Irradiation.....24  
 Humidity.....24

Conclusions.....26

References.....27

Appendix:  
 Computer Program ANTIREF for Calculating Three-layer.....31  
 Antireflection Coating Solutions.

Figures:

1. Two-layer Design Configuration..... 6

2. Theoretical Transmittance of Two-layer Design..... 6

3. Normalized Electric Field Intensity of Two-layer Design..... 6

4a. Antireflection Solutions for a Three-layer Design  
 with Fused Quartz as Substrate..... 9

4b. Antireflection Solutions for a Three-layer Design  
 with Calcium Fluoride as Substrate..... 9

5. Three-layer Design Configuration with Fused Quartz  
 as Substrate..... 9

6. Theoretical Transmittance of Three-layer Design  
 with Fused Quartz as Substrate..... 9

7. Normalized Electric Field Intensity of Three-layer  
 Design with Fused Quartz as Substrate.....10

8. Experimental Transmittance of Three-layer Design  
 with Fused Quartz as Substrate.....15

9a. Topography of AlN Single Layer.....17

9b. Cross Section of AlN Single Layer.....17

|     |                                     |
|-----|-------------------------------------|
| For |                                     |
| A&I | <input checked="" type="checkbox"/> |
| B   | <input type="checkbox"/>            |
| ced | <input type="checkbox"/>            |



| Availability Codes |                      |
|--------------------|----------------------|
| Dist               | Avail and/or Special |
| A-1                |                      |

|   |    |
|---|----|
| 10a. Topography of Al <sub>2</sub> O <sub>3</sub> Single Layer.....   | 17 |
| 10b. Cross Section of Al <sub>2</sub> O <sub>3</sub> Single Layer.....  | 17 |
| 11a. Topography of AlN/Al <sub>2</sub> O <sub>3</sub> /AlN Multilayer.....                                    | 17 |
| 11b. Cross Section of AlN/Al <sub>2</sub> O <sub>3</sub> /AlN Multilayer.....                                 | 17 |
| 12a. Enlargened Top View of AlN Single Layer Defect.....  | 18 |
| 12b. Enlargened Top View of Al <sub>2</sub> O <sub>3</sub> Single Layer Defect.....                           | 18 |
| 12c. Enlargened Top View of AlN/Al <sub>2</sub> O <sub>3</sub> /AlN Multilayer Defect.....                    | 18 |
| 13a. Damage Site 1 Showing Small Damage Craters<br>Amongst Defects.....                                       | 20 |
| 13b. Damage Site 2 Showing More and Larger Damage Craters<br>Amongst Defects (than Site 1).....               | 20 |
| 13c. Damage Site 3 Showing a Reduced Number of Apparent<br>Defects and More Damage Craters (than Site 2)..... | 20 |
| 13d. Damage Site 4 Showing Agglomeration of Damage Craters.....   | 20 |
| 13e. Damage Site 5 Showing Small Pitmarks and<br>Loss of Much of Outer Film.....                              | 20 |
| 14a. AES Spectrum of Smooth Film Portion of Site 2.....   | 22 |
| 14b. AES Spectrum Taken Within Damage Crater of Site 2.....   | 22 |
| 15. AES Spectrum of Smooth Film Portion of Site 4.....  | 23 |
| 16a. AES Profile of AlN Single Layer Exposed to Fluorine.....   | 25 |
| 16b. AES Profile of Al <sub>2</sub> O <sub>3</sub> Single Layer Exposed to Fluorine.....                      | 25 |

---

Tables:

|  |    |
|--|----|
| 1. Information on Samples Prepared in dc Magnetron System..... | 12 |
| 2. Information on Samples Prepared in rf Diode System.....     | 13 |
| 3. Purities of Materials Used in Sample Depositions.....       | 13 |
| 4. Laser Energy Densities for the Five Damage Sites.....       | 21 |

---

ACKNOWLEDGMENT

The authors would like to gratefully acknowledge the technical contributions of E. J. Ashley, A. D. Baer, R. Z. Dalbey, W. N. Faith, A. K. Green, J. L. Stanford, and R. W. Woolever. The authors would also like to thank P. J. Jaime for preparation of the manuscript. And lastly, the authors would like to acknowledge the Defense Advanced Research Projects Association (DARPA) for their partial support of this work.

## INTRODUCTION

New multilayer antireflective coatings are being developed for protective use on laser windows. These coatings consist of alternating layers of aluminum nitride and aluminum oxide, which are stable and scratch resistant. Both materials have large bandgaps and are highly transparent from the ultraviolet to the infrared, thus making them ideal for use with many laser systems.

Both two- and three-layer designs have been developed for use at certain wavelengths. The two-layer design was based upon the work of Cox and Hass (Reference 1) and uses aluminum oxide as the outer material. This is particularly desirable since  $Al_2O_3$  is resistant to moisture as well as to fluorine. The three-layer design was developed by applying the works of Baer and Mouchart who have determined techniques which allow for much design flexibility (References 2 and 3, respectively). This flexibility is the result of an extra degree of freedom which may be used to optimize the design with respect to low absorption, large bandwidth, good adherence, or ease of fabrication (Reference 4).

Preparations of the films have been achieved by numerous techniques including reactive sputtering and evaporation, chemical vapor deposition, ion plating, activated decomposition of organometallic compound vapors, aluminum anodization, and laser-assisted deposition during electron beam evaporation (References 5 through 36). In this study, the methods of dc magnetron, ion beam, and rf diode sputtering have been used to deposit single layers and multilayers. Films prepared by these techniques have typically been shown to be stoichiometric and of high packing density.

Studies on the reactions of the multilayer materials with fluorine, electron beam irradiation, and humidity as well as on their damage by laser radiation will be discussed. The main techniques used for analysis and characterization of the films after exposure to the above environments are scanning Auger microscopy (SAM), scanning electron microscopy (SEM), energy dispersive X-ray microanalysis (EDX), X-ray photoelectron spectroscopy (XPS), and Nomarski microscopy.

## MULTILAYER DESIGNS

The choice of materials, AlN and Al<sub>2</sub>O<sub>3</sub>, necessitate the use of multiple-layer design techniques for obtaining zero reflectance. Both materials have high transmittances at the wavelength of interest (i.e., 0.500μm), but by themselves cannot accomplish the reflectance requirement. These materials have been prepared with indices of refraction which allow for production of zero reflectance coatings.

Since quarter-wave designs which produce zero reflectance are not possible, general solutions to the two- and three-layer cases must be used. These solutions allow flexibility in the choices of layer thicknesses, which is very desirable from the standpoints of absorption in the layers and film preparation.

Absorption in the layers is a problem which normally must be accounted for when designing multilayer systems, but the design techniques utilized in this study do not include this factor. Thus, an indirect approach should be used such as optimizing the solution through manipulations of layer thicknesses (Reference 2).

## TWO-LAYER DESIGN

As discussed by Cox and Hass (Reference 1), for zero reflectance, when the multilayer consists of two layers whose thicknesses are not related by integral multiples of each other, one obtains:

$$\frac{\tan\phi_1}{\tan\phi_2} = - \frac{r_1 - r_3 + r_2(1 - r_1 r_3)}{r_1 - r_3 - r_2(1 - r_1 r_3)} \quad (1)$$

$$\text{and} \quad \tan\phi_1 \tan\phi_2 = \frac{r_1 + r_3 + r_2(1 + r_1 r_3)}{r_1 + r_3 - r_2(1 + r_1 r_3)} \quad (2)$$

$$\text{where} \quad \phi_j = \frac{2\pi n_j l_j}{\lambda} \quad \equiv \quad 2\pi X_j \quad ,$$

$$\text{and} \quad r_j = \frac{n_{j-1} - n_j}{n_{j-1} + n_j} \quad .$$

Note that  $n_j$  is the index of refraction of the  $j$ th layer,  $l_j$  is its thickness, and  $\lambda$  is the design wavelength.

Equations (1) and (2) may be written in the form:

$$X_1 = \frac{1}{2\pi} \tan^{-1} \left[ \pm \left( \frac{n_1^2(n_3-n_0)(n_2^2-n_0n_3)}{(n_1^2n_3-n_2^2n_0)(n_0n_3-n_1^2)} \right)^{1/2} \right] + \frac{m_1}{2} \quad (3)$$

$$\text{and } X_2 = \frac{1}{2\pi} \tan^{-1} \left[ \pm \left( \frac{n_2^2(n_3-n_0)(n_0n_3-n_1^2)}{(n_1^2n_3-n_2^2n_0)(n_2^2-n_0n_3)} \right)^{1/2} \right] + \frac{m_2}{2}, \quad (4)$$

where  $m_1 = 0, \pm 1, \pm 2, \dots$ ,

and  $m_2 = 0, \pm 1, \pm 2, \dots$ .

Thus, one may obtain a series of  $X_1$ 's and  $X_2$ 's and hence a series of physical thicknesses,  $l_1$ 's and  $l_2$ 's. Note that equations (3) and (4) imply four possible pairs of solutions for each  $m_1$  and  $m_2$  set, but in actuality only two of these pairs will satisfy equations (1) and (2).

Applying equations (3) and (4) to the present case of interest, where  $n_0=1.00$ ,  $n_1=1.60$ ,  $n_2=2.00$ ,  $n_3=1.46$  (these are the incident medium, outer aluminum oxide layer, inner aluminum nitride layer, and fused quartz substrate indices of refraction, respectively), and  $\lambda=0.500\mu\text{m}$ , a zero reflectance choice of thicknesses is then given by  $l_1=0.0631\mu\text{m}$  and  $l_2=0.0832\mu\text{m}$ . This configuration is shown in Figure 1. From this information, and assuming no absorption in the layers, normal light incidence, and constant indices of refraction for the wavelength region 0.3 to  $0.9\mu\text{m}$ , the transmission spectrum has been determined using a program developed by Loomis (Reference 37).

This spectrum is shown in Figure 2 as a function of wavelength. As can be seen, there is 100% transmission at  $0.500\mu\text{m}$  and a bandwidth of approximately  $0.06\mu\text{m}$  with a reflectance loss of 0.5% or less. The normalized electric field intensity as a function of depth into the layers is shown in Figure 3 and was determined by Elson (Reference 38). It is apparent that the electric field minimum occurs in the thicker aluminum nitride layer. This is advantageous from the standpoint that the aluminum nitride layer is the more absorbing material as shown by preliminary absorption measurements.

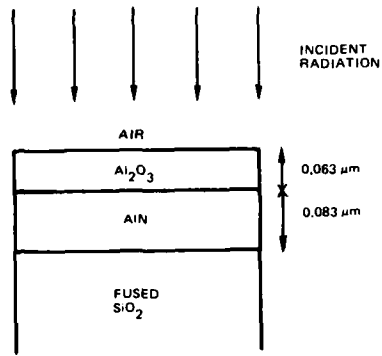


FIGURE 1. Two-layer Design Configuration.

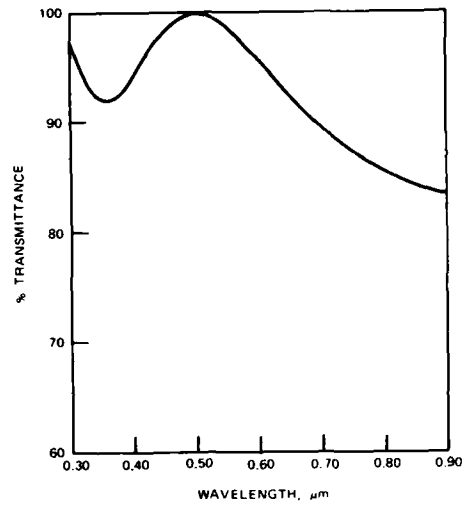


FIGURE 2. Theoretical Transmittance of Two-layer Design.

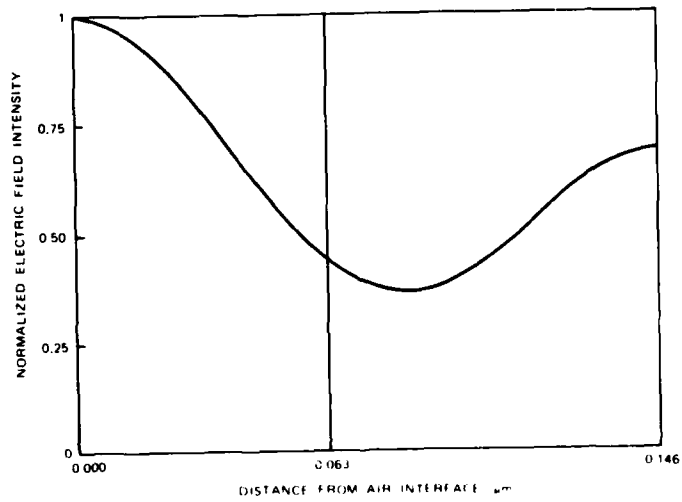


FIGURE 3. Normalized Electric Field Intensity of Two-layer Design.

## THREE-LAYER DESIGN

Based upon the works of Baer and Mouchart (References 2 and 3, respectively), an analytic solution for a general three-layer antireflective coating has been utilized. According to Baer, Smith's theorem may be used when determining what conditions must be applied to obtain zero reflectance. These conditions indicate that both the real and imaginary components of the Fresnel coefficients must vanish. Then, as discussed by Baer, one obtains:

$$X_1 = \pm \frac{1}{4\pi} \cos^{-1} \left[ \frac{r_2^2 + r_1^2 - |r_b|^2(1 + r_2^2 r_1^2)}{2r_2 r_1 (|r_b|^2 - 1)} \right] + \frac{m_1}{2}, \quad (5)$$

and 
$$X_2 = \frac{1}{4\pi} (\delta_a + \delta_b) + \frac{m_2}{2}, \quad (6)$$

where 
$$r_a = \frac{r_2 + r_1 \exp(-4\pi X_1 i)}{1 + r_2 r_1 \exp(-4\pi X_1 i)}, \quad (7)$$

$$r_b = \frac{r_3 + r_4 \exp(-4\pi X_3 i)}{1 + r_3 r_4 \exp(-4\pi X_3 i)}, \quad (8)$$

and 
$$X_j = \frac{n_j l_j}{\lambda}, \quad (9)$$

$$m_1 = 0, \pm 1, \pm 2, \dots,$$

$$m_2 = 0, \pm 1, \pm 2, \dots$$

Note that  $\delta_a$  and  $\delta_b$  refer to the phases of  $r_a$  and  $r_b$  respectively and that the  $X_j$  and  $r_j$  are as defined earlier. Hence, for a choice of  $X_3$ , and given the indices of refraction of the layers, one may obtain a series of solutions. Note that there are two series of solutions for each  $X_3$ .

A computer program in the language of Fortran has been written which calculates and then plots the solutions of  $X_1$  and  $X_2$  as functions of  $X_3$  given the indices of refraction and design wavelength. A listing of this program may be found in the Appendix.

Figure 4a shows a plot of  $X_1$  and  $X_2$  as functions of  $X_3$  for  $\lambda=0.500\mu\text{m}$ ,  $n_0=1.00$ ,  $n_1=2.00$ ,  $n_2=1.60$ ,  $n_3=2.00$ , and  $n_4=1.46$ . Figure 4b shows a similar plot with  $\lambda=0.500\mu\text{m}$ ,  $n_0=1.00$ ,  $n_1=2.00$ ,  $n_2=1.60$ ,  $n_3=2.00$ , and  $n_4=1.44$ . These indices of refraction correspond to the incident medium, aluminum nitride layer, aluminum oxide layer, aluminum nitride layer, and fused quartz substrate (Figure 4a) or calcium fluoride substrate (Figure 4b), respectively. Note that the solid curves correspond to the first solution and the dashed to the second.

A particular solution from the results shown in Figure 4a is  $X_3=0.250$ ,  $X_1=0.447$ , and  $X_2=0.326$ . Hence,  $l_1=0.112\mu\text{m}$ ,  $l_2=0.102\mu\text{m}$ , and  $l_3=0.625\mu\text{m}$ . This configuration is shown in Figure 5.

As in the two-layer case, a plot of the transmission spectrum as a function of wavelength is shown in Figure 6 (for the particular solution discussed above). Again, there is 100% transmission at  $0.500\mu\text{m}$  as expected, but the bandwidth at a reflectance loss of 0.5% is reduced to approximately  $0.02\mu\text{m}$ . Hence, from the standpoint of bandwidth, this design is not as desirable. The normalized electric field intensity is shown in Figure 7. In this case, the electric field minimum again occurs in one of the aluminum nitride layers, with the maximum occurring in the aluminum oxide layer. Thus, as in the two-layer case, the design appears to be a favorable choice from the standpoint of absorption.

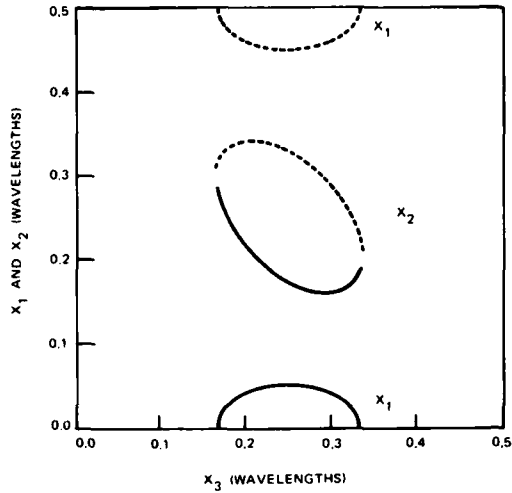


FIGURE 4. Antireflection Solutions for a Three-layer Design with Fused Quartz as Substrate. (a)

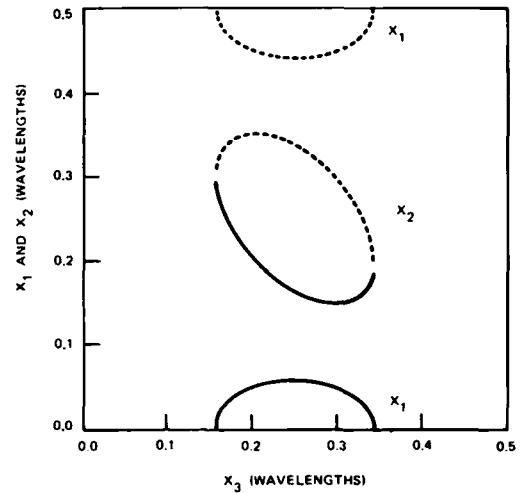


FIGURE 4. Antireflection Solutions for a Three-layer Design with Calcium Fluoride as Substrate. (b)

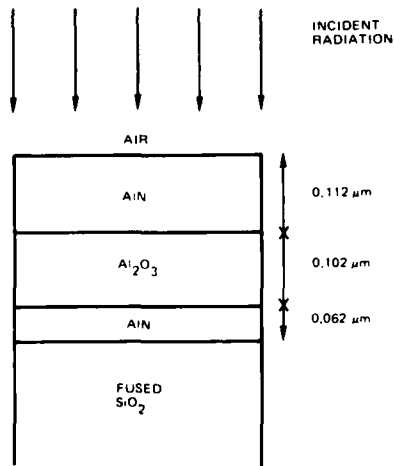


FIGURE 5. Three-layer Design Configuration with Fused Quartz as Substrate.

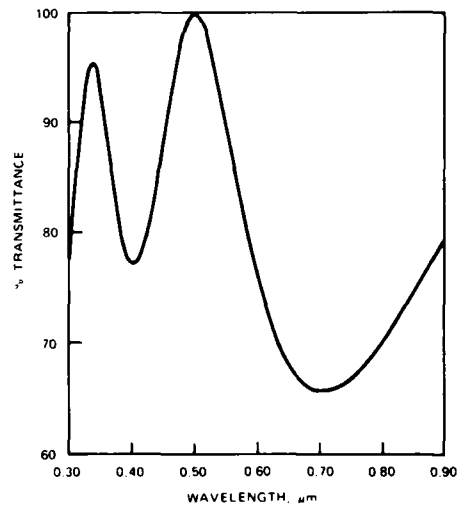


FIGURE 6. Theoretical Transmittance of Three-layer Design with Fused Quartz as Substrate.

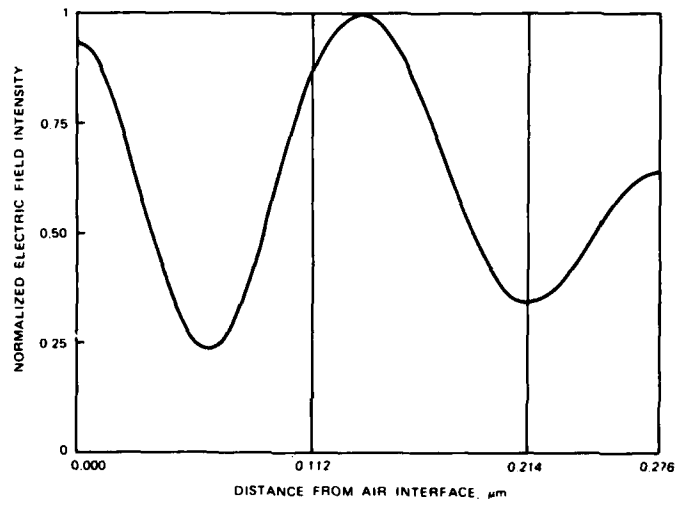


FIGURE 7. Normalized Electric Field Intensity of Three-layer Design with Fused Quartz as Substrate.

## SAMPLE PREPARATION

Several single-layer samples and one three-layer sample were deposited onto substrates of fused quartz, calcium fluoride, or silicon. Substrate diameters were 1 inch and thicknesses were 0.063 inch, 0.058 inch, and 0.023 inch, respectively. Very thin layers of Ag/Cr/Mo, Au/Cr/Mo, or Au/Cr were deposited onto some of the substrates prior to AlN or Al<sub>2</sub>O<sub>3</sub> deposition for the purpose of aiding in eliminating charging problems during analysis. Tables 1 and 2 contain lists of the specimens prepared along with any pertinent information relating to their depositions for depositions in the dc magnetron and rf diode sputtering systems, respectively. Approximate deposition temperatures for the two systems were 160°C and 300°C, respectively. Note that samples on Si or on aiding layers were used as witnesses. Sample M-177 of Al<sub>2</sub>O<sub>3</sub>, prepared in the ion beam sputtering system, was deposited on aiding layers of Au/Cr with a substrate of Si. The approximate gas pressure was  $1.5 \times 10^{-4}$  torr of Ar, deposition was at room temperature, and the estimated film thickness was 2800Å. Table 3 contains information regarding the purities of the materials used (for the various depositions) and their suppliers.

Most of the samples were deposited using a dc magnetron sputtering system with a 5-inch Varian sputter gun (samples listed with a "T" before their numbers; see Table 1). Some samples were prepared in a Randex model 2400 rf diode sputtering system (samples with an "S" before their numbers; see Table 2). One sample was prepared by ion beam deposition using an Ion Technology, Inc., 2.5mm ion gun (as indicated by an "M" before the sample number above).

TABLE 1. Information on Samples Prepared in dc Magnetron System.

| Sample Number | Film Material                                  | Aiding Layers | Approximate Gas Pressure (torr)                                      | Substrate        | Estimated Film Thickness (Å) |
|---------------|--|---------------|--|------------------|------------------------------|
| T-261S        | AlN  | -             | $3 \times 10^{-3} \text{N}_2$  | Fused Quartz     | 2030                         |
| T-265S        | AlN  | -             | $1.5 \times 10^{-3} \text{N}_2$<br>$1.5 \times 10^{-3} \text{Ar}$    | Si               | 2000                         |
| T-266S        | AlN  | Ag/Cr/Mo      | $3 \times 10^{-3} \text{N}_2$  | Fused Quartz     | 2000                         |
| T-268S        | AlN  | Ag/Cr/Mo      | $1.5 \times 10^{-3} \text{N}_2$<br>$1.5 \times 10^{-3} \text{Ar}$    | Fused Quartz     | 2000                         |
| T-270S        | Al <sub>2</sub> O <sub>3</sub>                 | -             | $3 \times 10^{-4} \text{O}_2$<br>$2.7 \times 10^{-3} \text{N}_2$     | Fused Quartz     | 2000                         |
| T-276S        | AlN  | -             | $1.5 \times 10^{-3} \text{N}_2$<br>$1.5 \times 10^{-3} \text{Ar}$    | CaF <sub>2</sub> | 2000                         |
| T-281S        | AlN  | -             | $3 \times 10^{-3} \text{N}_2$  | CaF <sub>2</sub> | 4000                         |
| T-289S        | (a) AlN<br>(outer)                             | -             | (a) $3 \times 10^{-3} \text{N}_2$                                    | Fused Quartz     | (a) 1120                     |
|               | (b) Al <sub>2</sub> O <sub>3</sub><br>(middle) | -             | (b) $3 \times 10^{-4} \text{O}_2$<br>$2.7 \times 10^{-3} \text{N}_2$ |                  | (b) 1020                     |
|               | (c) AlN<br>(inside)                            | -             | (c) $3 \times 10^{-3} \text{N}_2$                                    |                  | (c) 625                      |
| T-290S        | AlN  | Ag/Cr/Mo      | $3 \times 10^{-3} \text{N}_2$  | Fused Quartz     | 2000                         |
| T-290S        | AlN  | Au/Cr/Mo      | $3 \times 10^{-3} \text{N}_2$  | Fused Quartz     | 2000                         |
| T-297S        | AlN  | Au/Cr         | $3 \times 10^{-3} \text{N}_2$  | Si               | 2800                         |

TABLE 2. Information on Samples Prepared in rf Diode System.

| Sample Number | Film Material                  | Approximate Gas Pressure (torr)  | Substrate    | Film Thickness (Å) |
|---------------|--------------------------------|--|--------------|--------------------|
| S-826         | Al <sub>2</sub> O <sub>3</sub> | 8 x 10 <sup>-4</sup> O <sub>2</sub><br>7.2 x 10 <sup>-3</sup> N <sub>2</sub> | Fused Quartz | 2100               |
| S-827         | AlN                            | 2 x 10 <sup>-3</sup> N <sub>2</sub><br>6 x 10 <sup>-3</sup> Ar               | Fused Quartz | 7000               |
| S-833         | Al <sub>2</sub> O <sub>3</sub> | 8 x 10 <sup>-4</sup> O <sub>2</sub><br>7.2 x 10 <sup>-3</sup> Ar             | Fused Quartz | 2100               |
| S-834         | AlN                            | 2 x 10 <sup>-3</sup> N <sub>2</sub><br>6 x 10 <sup>-3</sup> Ar               | Fused Quartz | 7000               |
| S-835         | AlN                            | 8 x 10 <sup>-4</sup> N <sub>2</sub><br>7.2 x 10 <sup>-3</sup> Ar             | Fused Quartz | 7000               |

TABLE 3. Purities of Materials Used in Sample Depositions.

| Material                       | Purity (%) | Source                              |
|--------------------------------|------------|-------------------------------------|
| Al                             | 99.999     | Specialty Metals Division of Varian |
| Al <sub>2</sub> O <sub>3</sub> | Unknown    | Microelectronics Branch, NAVWPNCEN  |
| Au                             | 99.999     | American Smelting Company           |
| Mo                             | 99.999     | American Smelting Company           |
| Cr                             | 99.996     | Specialty Metals Division of Varian |

The three-layer sample was prepared according to the 0.500 $\mu$ m design discussed previously (particular solution). Indices were assumed to be 2.00 and 1.60 for AlN and Al<sub>2</sub>O<sub>3</sub>, respectively, and the materials were deposited until the necessary thicknesses had been obtained. Although the indices of refraction have not been accurately determined in this study, many researchers have previously determined them to range from 1.70-2.15 for AlN and 1.42-1.79 for Al<sub>2</sub>O<sub>3</sub> (References 5, 6, 16, 23, 25, 26, 28, 29, 30, 35, and 36), implying that the assumed values are realistic. Furthermore, recent laboratory studies indicate that the assumed indices are more likely.

A transmission spectrum of the three-layer sample coating over the wavelength region of 0.3 to 0.9 $\mu$ m was measured using a Beckman DU-7 UV/VIS spectrophotometer. This spectrum is shown in Figure 8. In comparison to the theoretical spectrum shown in Figure 6, it is apparent that the two are similar in curve shape, but some additional tuning is necessary in the experimental sample preparation to more closely approximate the theoretical curve. The experimental maximum in transmission of 98.8% occurred at 0.553 $\mu$ m. By the use of a program written by Loomis (Reference 37), variations in the thicknesses and indices of the layers were made to attempt to determine what changes would cause a calculated transmission spectrum to approach the appearance of the experimental spectrum. It was found that the differences between the two spectra is a combination of a need to determine the actual film indices and to measure more accurately the deposition rates of the materials. At this time, efforts are being made to accomplish these tasks.

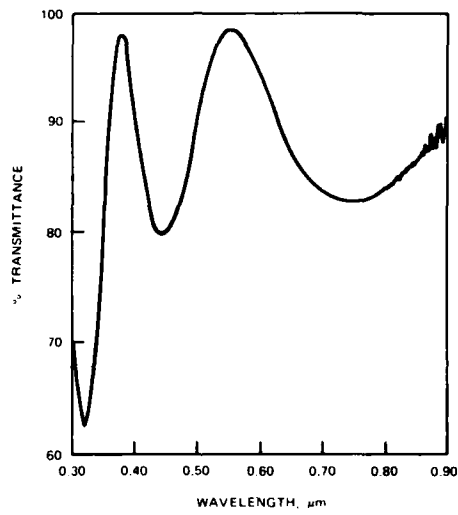


FIGURE 8. Experimental Transmittance of Three-layer Design with Fused Quartz as Substrate.

## FILM STRUCTURE

Study of the structures of both single and multilayer films were made using a scanning electron microscope. The films were coated with thin layers of Au (approximately 150Å) to avoid charging problems.

Shown in Figures 9a and 9b are typical top and cross-sectional views of an AlN single layer. This film was sample number T-297S prepared in the dc magnetron system. Figures 10a and 10b show top and cross-sectional views of an Al<sub>2</sub>O<sub>3</sub> single layer prepared in the ion beam system (sample M-177). Figures 11a and 11b show top and cross-sectional views of the AlN/Al<sub>2</sub>O<sub>3</sub>/AlN multilayer (sample T-289S) prepared in the dc magnetron system. In the last case, the three layers can be distinguished.

Many defects are apparent on the surface of the AlN single and multilayer films. It is not known at this time whether the defects are growth defects of a nodular type or whether they are bubbles or splatters on the surfaces only. These defects are typically on the order of 5-10µm in diameter. The Al<sub>2</sub>O<sub>3</sub> specimen is of a much finer surface structure, although smaller defects (approximately 1µm in diameter) are apparent on it also. Figures 12a through 12c show magnified views of the AlN, Al<sub>2</sub>O<sub>3</sub>, and multilayer defects, respectively.

The cross sections or side views of the AlN layers display columnar growth type structures. It has been determined by transmission electron diffraction that these films are polycrystalline. The side views of the Al<sub>2</sub>O<sub>3</sub> layers show much smoother textures, with no columnar growth structures apparent at the magnifications achieved in these experiments. A pattern was not obtained from the diffraction studies for the Al<sub>2</sub>O<sub>3</sub>, and hence it is probably amorphous. Note that the Al<sub>2</sub>O<sub>3</sub> single layer and multilayer specimens were prepared in different sputtering systems, but the texture of the Al<sub>2</sub>O<sub>3</sub> still remains similar in the two cases.

From electron spectroscopy for chemical analysis (ESCA) studies, AlN materials have been determined to be 95% stoichiometric with the remainder consisting mostly of Al<sub>2</sub>O<sub>3</sub>. Al<sub>2</sub>O<sub>3</sub> films have been shown to be 99% stoichiometric.

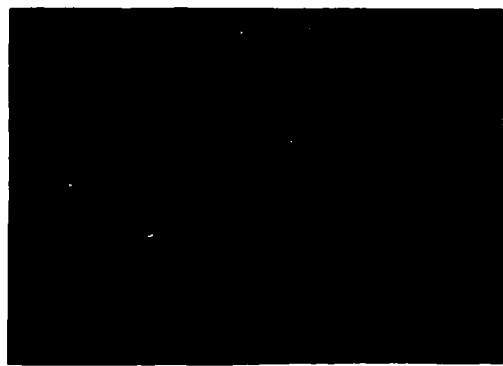


FIGURE 9. Topography of AlN Single Layer.  
(a)



FIGURE 9. Cross Section of AlN Single Layer.  
(b)



FIGURE 10. Topography of Al<sub>2</sub>O<sub>3</sub> Single Layer.  
(a)



FIGURE 10. Cross Section of Al<sub>2</sub>O<sub>3</sub> Single Layer.  
(b)

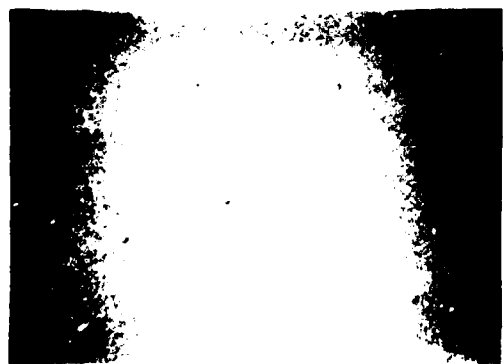


FIGURE 11. Topography of AlN/Al<sub>2</sub>O<sub>3</sub>/AlN Multilayer.  
(a)



FIGURE 11. Cross Section of AlN/Al<sub>2</sub>O<sub>3</sub>/AlN Multilayer.  
(b)



FIGURE 12. Enlarged Top View of AlN Single Layer Defect.  
(a)

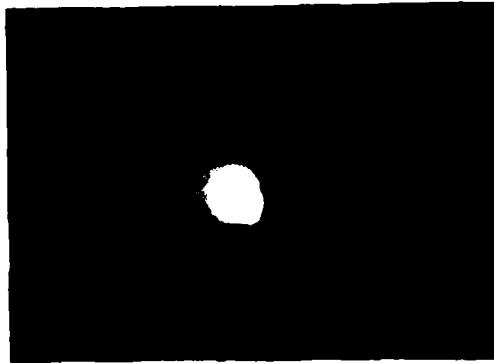


FIGURE 12. Enlarged Top View of Al<sub>2</sub>O<sub>3</sub> Single Layer Defect.  
(b)

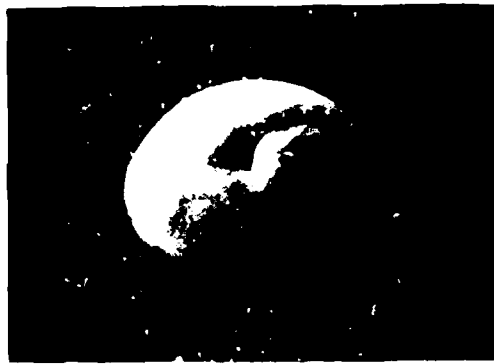


FIGURE 12. Enlarged Top View of AlN/Al<sub>2</sub>O<sub>3</sub>/AlN Multilayer Defect.  
(c)

## RESULTS

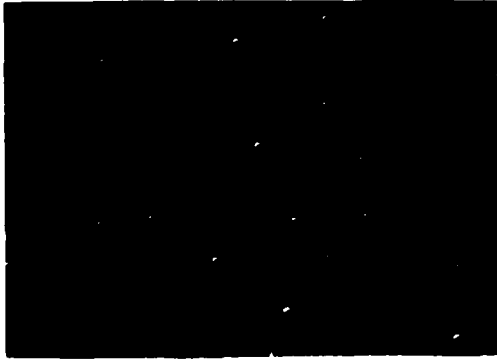
Results have been obtained on sample behavior following exposure to laser radiation, fluorine, electron beam irradiation, and humidity. The samples studied were discussed earlier, and will be referred to by their designated sample numbers. Not all samples given earlier will be discussed since some were only used for obtaining preliminary spectral information and since experimental difficulties were encountered during analysis with others which were associated with film quality and charging problems.

## LASER RADIATION

The effects of laser radiation on the multilayer sample were studied with a Phi 600 scanning Auger microscopy system (after damage). The sample surface was cleaned during analysis by sputtering with Ar ions using an accelerating voltage of 4kV. For SiO<sub>2</sub>, an approximate removal rate has been determined to be 40Å/min.

A pulsed dye laser in a triaxial configuration was utilized for damaging the film at a wavelength of 0.497 $\mu$ m. The first step in the laser damage study was to scratch crosshairs onto the film on opposite sides of its center along a sample diagonal. These crosshairs were then used as index marks for locating five equally spaced sites between them. Each site was then irradiated in air with a few laser pulses of increasing energy density. The pulse shape was a 1mm diameter flat top ( $\pm$  5% flatness) with a duration of 0.55 $\mu$ s. Film breakdown thresholds were roughly determined by observing the beginning of film changes with a video microscopy system (VIMS). Note that no attempts were made in this study to determine actual damage thresholds of the materials. The main purpose of this study was to determine the behavior of the film after exposure to laser radiation.

Table 4 lists the energy density of each shot for the five sites. Shown in Figures 13a through 13e are portions of the centers of each of the five sites. These figures in comparison to a typical undamaged site (such as that in Figure 11a) show an increasing number of damage craters with respect to defects for an increasing energy density. Site 1 shows mostly defects plus some small damage craters. Sites 2 and 3 show more and larger damage craters with a reduced number of apparent defects. Site 4 shows the beginning of damage crater agglomeration, and Site 5 shows many small pit marks which appear to lay at the centers of what were originally damage craters (the pits are at the centers of circular patterns which resemble agglomerated craters). In addition, for Site 5, it is apparent that there is a loss of much of the outer film.



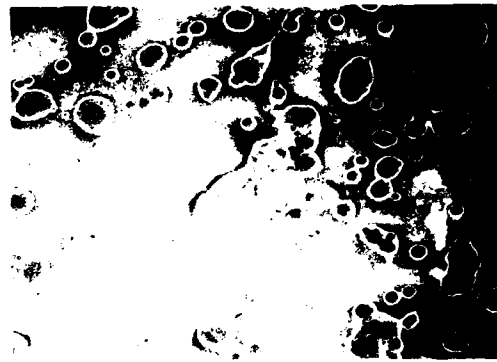
100μ  
FIGURE 13. Damage Site 1 Showing Small  
Damage Craters Amongst Defects.  
(a)



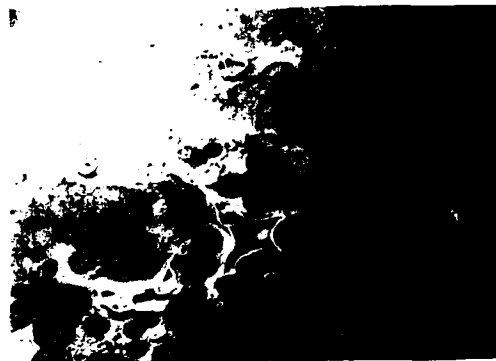
100μ  
FIGURE 13. Damage Site 2 Showing More and Larger  
Damage Craters Amongst Defects (than Site 1).  
(b)



100μ  
FIGURE 13. Damage Site 3 Showing a Reduced Number of  
Apparent Defects and More Damage Craters (than Site 2).  
(c)



100μ  
FIGURE 13. Damage Site 4 Showing  
Agglomeration of Damage Craters.  
(d)



100μ  
FIGURE 13. Damage Site 5 Showing Small Pitmarks and Loss of Much of Outer Film.  
(e)

TABLE 4. Laser Energy Densities for the Five Damage Sites.

|           | Energy Density (J/cm <sup>2</sup> ) |        |        |        |        |
|-----------|-------------------------------------|--------|--------|--------|--------|
|           | Site 1                              | Site 2 | Site 3 | Site 4 | Site 5 |
| 1st pulse | 3.2                                 | 9.2    | 12.    | 20.    | 50.    |
| 2nd pulse | 5.9                                 | 9.2    | -      | -      | -      |
| 3rd pulse | 9.4                                 | -      | -      | -      | -      |

The approximate number of defects for typical portions of the film where no damage was done is 70 (see the sampling area of Figure 11a for an example). For Sites 1 and 2, the number of damage craters plus defects which did not damage are approximately 60 and 70 (in the same size sampling area), respectively. These are similar to that of the undamaged site, which implies that damage is initiating at defects. For Sites 3 through 5, the number of craters plus undamaged defects is large in comparison to the number of defects on the undamaged site, increasing in number with increasing energy density (assuming the pit marks of Site 5 are indeed the centers of what were originally damage craters), although few apparent defects remain on the sites. These results support damage initiating at the defect sites, with some other possible mode(s) of damage (e.g., caused by non-observable defects) also contributing to the cratering.

Auger spectra were obtained for some of the damage sites. Thin layers of gold were deposited on the films prior to the study and then removed by Ar ion sputtering (as discussed earlier) just until Auger peaks corresponding to the underlying film were obtained. Figures 14a and 14b show spectra obtained at Site 2. Figure 14a illustrates a portion of the damage site which appeared to be unaffected by the laser radiation (herein referred to as smooth film) and Figure 14b was taken within a damage crater. It is apparent that the smooth film consists mostly of AlN and the crater site consists of AlN plus Al<sub>2</sub>O<sub>3</sub>. Similar spectra were obtained for some of the other sites, where the spectra from the craters always showed an increase in Al<sub>2</sub>O<sub>3</sub> with respect to AlN. In addition, when comparing damage sites, it is apparent that the amount of Al<sub>2</sub>O<sub>3</sub> with respect to AlN increased with increasing energy density. Figure 15 shows the spectrum obtained on a smooth portion of the film at Site 4. A possible explanation for the growth of the oxide peak is the dissociation of some of the surface AlN, and then combination of the Al with oxygen to form Al<sub>2</sub>O<sub>3</sub> (recall that these studies were performed in air). Thus, the amount of oxidation of AlN would increase with energy density. In addition, the larger oxide peaks in the craters may be explained by assuming that these are positions on the film where the energy was absorbed more, or not conducted away as quickly, hence resulting in temperature buildup and more oxidation.

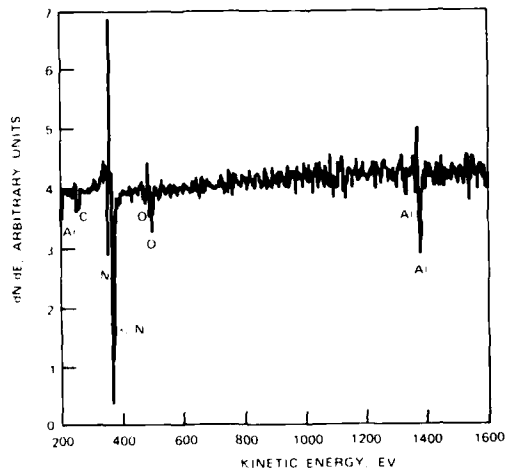


FIGURE 14. AES Spectrum of Smooth Film Portion of Site 2.  
(a)

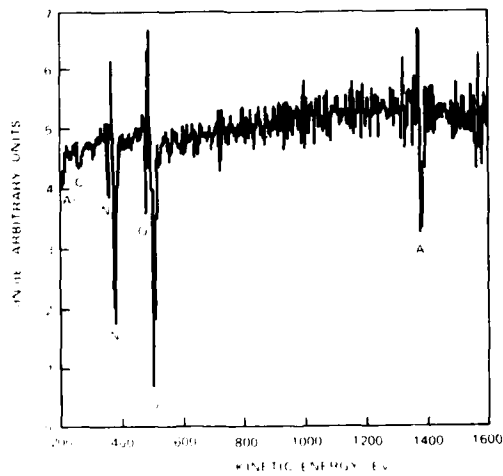


FIGURE 14. AES Spectrum Taken Within Damage Crater of Site 2.  
(b)

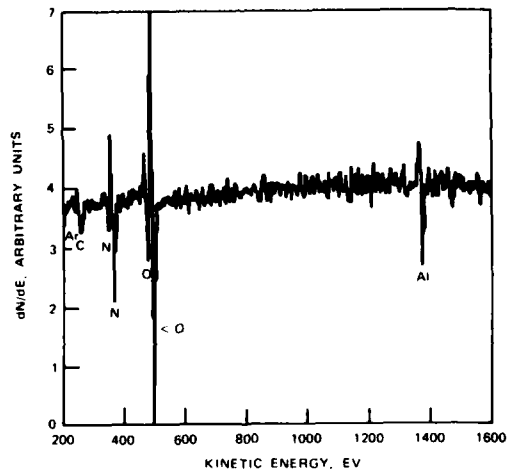


FIGURE 15. AES Spectrum of Smooth Film Portion of Site 4.

## FLUORINE EXPOSURE

Single layer samples T-297S and M-177 of AlN and Al<sub>2</sub>O<sub>3</sub>, respectively, were exposed to 10% HF in Ar for 1 hour, and were then examined for fluorine penetration.

EDX was initially used to detect the fluorine. Since this technique examines the constituents of the materials to a much greater depth (on the order of a micron) than a technique such as AES, any severe fluorine penetration should be detected. Fluorine was not detected in either the AlN or Al<sub>2</sub>O<sub>3</sub>. Hence, either the fluorine had not penetrated the material to a very great depth, or the fluorine concentration was low (low atomic number materials have low X-ray intensities due to low fluorescence yield and high sample absorption; see Reference 39).

AES and XPS were then used to analyze the film makeup since the results of the EDX had indicated no great depth penetration of the fluorine in either film. With these techniques, fluorine was observed. Figures 16a and 16b display AES profiles of the AlN and Al<sub>2</sub>O<sub>3</sub> films, respectively. Note that the AES system used in this case is a Physical Electronics 548 Auger/ESCA system, which employed a 1kV beam of Ar ions for sputter removal. For SiO<sub>2</sub>, a removal rate of 15Å/min. is typical. Assuming this rate for AlN and Al<sub>2</sub>O<sub>3</sub> yields approximate depth penetrations of 30-45Å for both films, although the fluorine appears to drop off (with depth) at a slightly higher rate in the Al<sub>2</sub>O<sub>3</sub> film.

## ELECTRON BEAM IRRADIATION

During surface studies such as SEM and SAM, physical changes of the AlN and Al<sub>2</sub>O<sub>3</sub> films were observed. Dark spots indicating changes in electron yields were observed at positions on the films where the electron beams were concentrated. At this time it is uncertain whether these changes were temporary (i.e., caused by contaminants being deposited on or removed from the film surfaces) or permanent. It is important to note that, as discussed earlier, it was necessary to coat the films with thin layers of a conducting material such as Au to avoid charging problems.

## HUMIDITY

Single layer samples T-297S and M-177 of AlN and Al<sub>2</sub>O<sub>3</sub>, respectively (several sister samples were produced, resulting in the availability of a "fresh" sample for each study), were exposed to 95% relative humidity at 60°C for 24 hours. With the use of a Nomarski microscope, no change in the Al<sub>2</sub>O<sub>3</sub> sample was observed although the AlN showed signs of degradation.

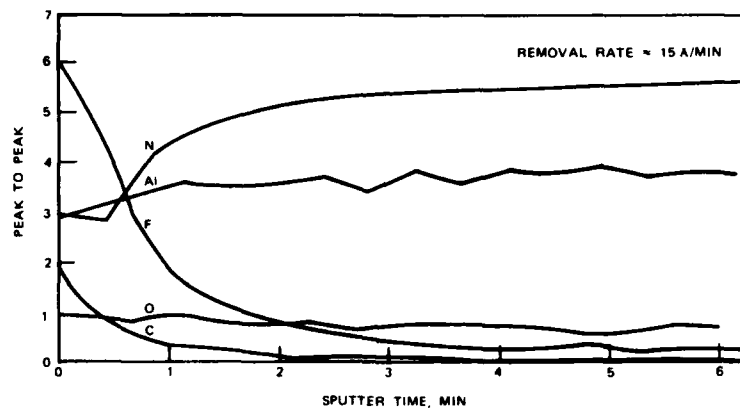


FIGURE 16. AES Profile of AlN Single Layer Exposed to Fluorine. (a)

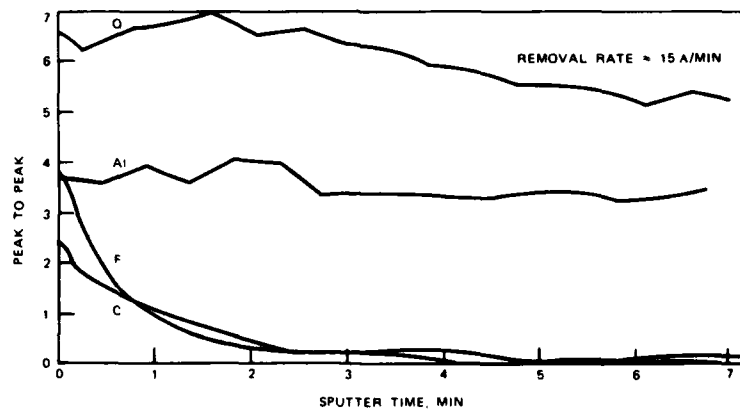


FIGURE 16. AES Profile of Al<sub>2</sub>O<sub>3</sub> Single Layer Exposed to Fluorine. (b)

## CONCLUSIONS

The theoretical aspects of the AlN/Al<sub>2</sub>O<sub>3</sub> multilayer designs indicate that perhaps the two-layer case may be more useful because of its bandwidth. At a reflectance loss of 0.5%, it has a bandwidth three times the size of that of the three-layer design. Although it has not been discussed in this study, simple calculations show that a two-layer quarter wave design is possible with a low reflectance (less than 0.005). This may be a more practical design. In this study, a film corresponding to the three-layer design was prepared and transmission results indicated a need to determine more accurately the indices of refraction and deposition rates of the materials.

Film structure studies indicate that defects are apparent on both the AlN, Al<sub>2</sub>O<sub>3</sub>, and AlN/Al<sub>2</sub>O<sub>3</sub>/AlN multilayer samples. The defects on the Al<sub>2</sub>O<sub>3</sub> appear to be smaller (approximately 1 $\mu$ m in diameter as compared with 5-10 $\mu$ m for the AlN single and multilayer films). The growth structure of the AlN is columnar, whereas that of the Al<sub>2</sub>O<sub>3</sub> is much smoother (no structure is observed at the SEM magnifications used in this study).

Laser damage studies indicate that multilayer damage initiates predominantly at defect sites. In addition, SAM studies indicate that the AlN outer layer of the multilayer oxidizes upon exposure to laser radiation in air. The amount of oxidation increases with increasing laser energy density and is also greater within damage craters than on portions of the film which appear to be unaffected by the laser radiation.

Fluorine exposure studies show depth penetrations of approximately 30-45 $\text{\AA}$  (assuming the same sputter removal rate of AlN and Al<sub>2</sub>O<sub>3</sub> as SiO<sub>2</sub>) in both films with the fluorine dropping off with depth at a slightly higher rate in the Al<sub>2</sub>O<sub>3</sub>.

Surface analysis techniques such as SEM and SAM indicate a sensitivity of the films to the electron beams. It is not certain whether the film changes after electron beam exposure are permanent.

After exposure to humidity, an Al<sub>2</sub>O<sub>3</sub> single-layer film underwent no observable change, although a AlN single-layer film exposed to the same condition degraded.

Most importantly, it is apparent that the use of an AlN/Al<sub>2</sub>O<sub>3</sub> multilayer in the environments described above dictates that Al<sub>2</sub>O<sub>3</sub> should be the outer material.

Overall, both films appear to be durable and relatively easy to prepare as a multilayer system. These studies are continuing and clean room techniques are being applied to achieve films with fewer defects.

## REFERENCES

1. J. T. Cox and G. Hass. "Antireflection Coating for Optical and Infrared Optical Materials," in *Physics of Thin Films*, Vol. 2, ed. by G. Hass and R. E. Thun. New York, Academic Press, 1964. Pp. 239-304.
2. A. D. Baer. "Design of Three-Layer Antireflection Coatings," presented at *Laser Induced Damage in Optical Materials: 1976*, Boulder, Co., 13-15 July 1976, in *NBS Spec. Publ. 462*, ed. by A. J. Glass and A. H. Guenther. December 1976. Pp. 221-229.
3. J. Mouchart. "Thin Film Optical Coatings. 2: Three-Layer Antireflection Coating Theory," *Applied Optics*, Vol. 16, No. 10 (October 1977), pp. 2722-2728.
4. Hughes Research Laboratories. *Exploratory Development on Antireflective Coating for 2 to 6 Micrometers for Fluorine Windows*, by J. E. Rudisill. Malibu, Calif., Hughes Research Laboratories, March 1978. 78 pp. (Hughes Research Laboratories AFML-TR-78-19.)
5. J. Duchene. "Radiofrequency Reactive Sputtering for Deposition of Aluminum Nitride Thin Films," *Thin Solid Films*, Vol. 8 (1971), pp. 69-79.
6. United Aircraft Corporation Research Laboratories. *Sputtered Thin Film Research*, by A. J. Shuskus, D. J. Quinn, E. L. Paradis, J. M. Berak, and D. E. Cullen. East Hartford, Ct., United Aircraft Corporation Research Laboratories, October 1973. 59 pp. (United Aircraft Corporation Research Laboratories M951337-9, AD-769972.)
7. United Aircraft Corporation Research Laboratories. *Sputtered Thin Film Research*, by A. J. Shuskus, D. J. Quinn, E. L. Paradis, J. M. Berak, D. E. Cullen, and T. M. Reeder. East Hartford, Ct., United Aircraft Corporation Research Laboratories, November 1974. 211 pp. (United Aircraft Corporation Research Laboratories N921337-15, AD/A-003005.)
8. N. Lieske and R. Hezel. "Formation of Al-Nitride Films at Room Temperature by Nitrogen Ion Implantation Into Aluminum," *J. Appl. Phys.*, Vol. 52, No. 9 (September 1981), pp. 5806-5810.
9. J. J. Hantzpergue, Y. Pauleau, J. C. Remy, O. Roptin, and M. Coiller. "Electrical Properties of Sputtered AlN Films and Interface Analyses by Auger Electron Spectroscopy," *Thin Solid Films*, Vol. 75 (1981), pp. 167-176.

10. Y. Murayama, K. Kashiwagi, M. Kikuchi. "Aluminum Nitride Films by rf Reactive Ion Plating," J. Vac. Sci. Technol., Vol. 17, No. 4 (July/August 1980), pp. 796-799.
11. RCA Laboratories. Piezoelectric Aluminum Nitride Films, by M. T. Duffy and C. C. Wang. Princeton, NJ, RCA Laboratories, October 1974. 139 pp. (RCA Laboratories PRRL-74-CR-65, AD-A007657.)
12. J. K. Liu, K. M. Lakin, and K. L. Wang. "Growth Morphology and Surface-Acoustic-Wave Measurements of AlN Films on Sapphire," J. Appl. Phys., Vol. 46, No. 9 (September 1975), pp. 3703-3706.
13. K. M. Lakin, J. K. Liu, and K. L. Wang. "Abstract: Growth Morphology and Surface-Acoustic-Wave Measurements of AlN Films on Sapphire," J. Vac. Sci. Technol., Vol. 13, No. 1 (January/February 1976), pp. 37-38.
14. University of Southern California, Electronic Sciences Laboratory. Aluminum Nitride for Surface Acoustic Waves, by K. M. Lakin. Los Angeles, Calif., University of Southern California, Electronic Sciences Laboratory, August 1974. 37 pp. (AD/A-002138.)
15. F. Takeda, T. Mori, and T. Takahashi. "Effect on Hydrogen Gas on c-Axis Oriented AlN Films Prepared by Reactive Magnetron Sputtering," Japanese J. Appl. Phys., Vol. 20, No. 3 (March 1981), pp. L169-L172.
16. E. V. Gerova, N. A. Ivanov, and K. I. Kirov. "Deposition of AlN Thin Films by Magnetron Reactive Sputtering," Thin Solid Films, Vol. 81 (1981), pp. 201-206.
17. K. M. Lakin, J. S. Wang, and A. R. Landin. "Aluminum Nitride Thin Film and Composite Bulk Wave Resonators," in 36th Annual Frequency Control Symposium, 1982. Pp. 517-524. (AD P001565.)
18. A. Fathimulla and A. A. Lakhani. "Reactively rf Magnetron Sputtered AlN Films as Gate Dielectric," J. Appl. Phys., Vol. 54, No. 8 (August 1983), pp. 4586-4589.
19. J. R. Rairden. "Aluminum Nitride Thin Films Deposited by Reactive Evaporation," in Thin Film Dielectrics Symposium, ed. by F. Vranty. New York, NY, Electrochem. Soc., Inc., 1969. Pp. 279-285.
20. H. Yamashita, K. Fukui, S. Misawa, and S. Yoshida. "Optical Properties of AlN Epitaxial Thin Films in the Vacuum Ultraviolet Region," J. Appl. Phys., Vol. 50, No. 2 (February 1979), pp. 896-898.

21. S. Winształ, B. Wnuk, H. Majewska-Minor, T. Niemyski. "Aluminum Nitride Thin Films and Their Properties," *Thin Solid Films*, Vol. 32 (1976), pp. 251-254.
22. S. Mirsch and H. Reimer. "Preparation and Electrical Properties of Al-AlN-Si Structures," *Phys. Stat. Sol.(a)*, Vol. 11 (1972), pp. 631-635.
23. N. Puychevriier and M. Menoret. "Synthesis of III-V Semiconductor Nitrides by Reactive Cathodic Sputtering," *Thin Solid Films*, Vol. 36 (1976), pp. 141-145.
24. A. J. Noreika and M. H. Francombe. "Structural, Optical and Dielectric Properties of Reactively Sputtered Films in the System AlN-BN," *J. Vac. Sci. Technol.*, Vol. 6, No. 4 (July 1969), pp. 722-726.
25. J. Bauer, L. Biste, and D. Bolze. "Optical Properties of Aluminum Nitride Prepared by Chemical and Plasmachemical Vapour Deposition," *Phys. Stat. Sol.(a)*, Vol. 39 (1977), pp. 173-181.
26. M. T. Duffy and W. Kern. "Chemical Vapor Deposition of Aluminum Oxide Films from Organo-Aluminum Compounds," *RCA Review*, Vol. 31, No. 4 (December 1970), pp. 754-770.
27. V. J. Silvestri, C. M. Osburn, and D. W. Ormond. "Properties of Al<sub>2</sub>O<sub>3</sub> Films Deposited from the AlCl<sub>3</sub>, CO<sub>2</sub>, and H<sub>2</sub> System," *J. Electrochem. Soc.: Solid-State Science and Technology*, Vol. 125, No. 6 (June 1978), pp. 902-907.
28. E. Ferrieu and B. Pruniaux. "Preliminary Investigations of Reactively Evaporated Aluminum Oxide Films on Silicon," *J. Electrochem. Soc.: Solid State Science*, Vol. 116, No. 7 (July 1969), pp. 1008-1013.
29. C. A. T. Salama. "RF Sputtered Aluminum Oxide Films on Silicon," *J. Electrochem. Soc.: Solid State Science*, Vol. 117, No. 7 (July 1970), pp. 913-917.
30. M. G. Mier and E. A. Buvinger. "A Comparative Study of Anodized, Evaporated, and Sputtered Aluminum Oxide Thin Films," *J. Vac. Sci. Technol.*, Vol. 6, No. 4 (1969), pp. 727-730.
31. S. O. Kanstad and P. E. Nordal. "Infrared Photoacoustic Spectroscopy of Solids and Liquids," *Infrared Physics*, Vol. 19, No. 3-4 (August 1979), pp. 413-422.

32. R. R. Hart, F. W. Reuter III, H. P. Smith Jr., and J. M. Khan. "Oxygen K-shell X-ray Production in Thin Films of Aluminum Oxide by 20- to 100- keV Photons," *Physical Review*, Vol. 179, No. 1 (5 March 1969), pp. 4-9.
33. C. H. Chen and J. Silcox. "Surface Guided Modes in an Aluminum Oxide Thin Film," *Solid State Communications*, Vol. 17 (1975), pp. 273-275.
34. A. Ya. Vyatskin and V. V. Trunev. "The Interaction of Electrons with Thin Films of Dielectrics," *Radiotekh. Elektron*, Vol. 17, No. 9 (1972), pp. 1899-1905.
35. V. F. Korzo. "Preparation of Thin Layers of Aluminum Oxide by Pyroactivated Decomposition of Organic Compounds," *Zhurnal Prikladnoi Khimii*, Vol. 49, No. 1 (January 1975), pp. 74-77.
36. Northrop Research and Technology Center. *Laser-Assisted Deposition Coatings*, by J. M. Rowe. Palos Verdes Peninsula, Calif., Northrop Research and Technology Center, September 1983. 76 pp. (Northrop Research and Technology Center AFWL-TR-83-34.)
37. Air Force Weapons Laboratory. *Computing the Optical Properties of Multilayer Coatings*, by J. S. Loomis. Kirtland Air Force Base, NM, Air Force Weapons Laboratory, September 1975, 30 pp. (Air Force Weapons Laboratory AFWL-TR-75-202.)
38. The calculation of field dependence was performed by J. M. Elson.
39. Princeton Gamma-Technology, Inc. *Electron Probe Microanalysis Using Energy Dispersive X-ray Spectroscopy*, by N. C. Barbi. Princeton, NJ., Princeton Gamma-Technology, Inc.

APPENDIX

COMPUTER PROGRAM ANTIREF FOR CALCULATING  
THREE-LAYER ANTIREFLECTION COATING SOLUTIONS

The following program calculates the thickness solutions for zero reflectance from a three-layer thin film system (based upon the work of Baer; reference 2).

```
C ANTIREF.FOR
C
C
C LESLIE G. KJSHIGGE
C
C
C APRIL 9, 1984
C
C THIS PROGRAM CALCULATES THE THICKNESS SOLUTIONS FOR ZERO
C REFLECTANCE FROM A THREE LAYER THIN FILM SYSTEM BASED UPON
C THE WORK OF A.D. BAER (REPORT ON MULTILAYER FILM PROGRAM FOR
C JULY, 1976 - SEPT., 1977; NAVAL WEAPONS CENTER, CHINA LAKE,
C CALIFORNIA). THE FILM IS ASSUMED TO BE LOSSLESS AND CERTAIN
C INPUT PARAMETERS ARE REQUIRED (WAVELENGTH OF RADIATION AND
C INDICES OF REFRACTION):
C
C
C THE OPTICAL THICKNESSES FOR LAYERS ONE AND TWO (OUTER AND
C MIDDLE LAYERS, RESPECTIVELY) ARE PLOTTED AGAINST THAT FOR THE
C THIRD LAYER (ON SUBSTRATE). THUS, THE USER MAY CHOOSE A
C DESIRABLE THIRD LAYER THICKNESS AND READ OFF THE THICKNESSES
C NECESSARY FOR THE OTHER LAYERS. NOTE THAT THERE ARE TWO
C SOLUTIONS FOR THE FIRST AND SECOND LAYER THICKNESSES FOR
C EVERY THIRD LAYER THICKNESS (WHERE A SOLUTION IS POSSIBLE).
C THESE SOLUTIONS ARE DISTINGUISHED BY SOLID AND DASHED LINES.
C ALSO NOTE THAT SOLUTIONS EXIST FOR EVERY MULTIPLE OF A HALF-
C WAVE FOR THE OPTICAL THICKNESSES.
C
C
C THE PHYSICAL THICKNESSES ARE NOT CALCULATED IN THIS PROGRAM,
C ALTHOUGH THEY MAY BE DETERMINED FROM:
C  $TI = (XI * WVLGTH) / NI,$ 
C WHERE TI DENOTES THE THICKNESS OF LAYER I, XI DENOTES THE
C OPTICAL THICKNESS OF LAYER I, WVLGTH DENOTES THE WAVELENGTH
C OF THE INCIDENT RADIATION, AND NI DENOTES THE INDEX OF REFRACTION OF LAYER I.
C
```

Following  
Reproduced from  
best available copy. 6  
PG. 5

NWC TP 6651

```

C
C DEFINITION OF PARAMETERS:
C   WVLGTH = WAVELENGTH OF IMPINGENT RADIATION (FREE SPACE),
C           MICRONS,
C   N0 = INDEX OF REFRACTION OF ATMOSPHERE,
C   N1 = INDEX OF REFRACTION OF LAYER 1,
C   N2 = INDEX OF REFRACTION OF LAYER 2,
C   N3 = INDEX OF REFRACTION OF LAYER 3,
C   N4 = INDEX OF REFRACTION OF SUBSTRATE,
C   R10 = FRESNEL COEFFICIENT BETWEEN LAYER 1 AND ATMOSPHERE,
C   R21 = FRESNEL COEFFICIENT BETWEEN LAYERS 2 AND 1,
C   R23 = FRESNEL COEFFICIENT BETWEEN LAYERS 2 AND 3,
C   R34 = FRESNEL COEFFICIENT BETWEEN LAYERS 3 AND 4,
C   RA = FRESNEL COEFFICIENT BASED ON SMITH'S THEOREM,
C   RB = FRESNEL COEFFICIENT BASED ON SMITH'S THEOREM,
C   RBMAG = MAGNITUDE OF RB,
C   DELPA = PHASE OF RA (SOLID SOLUTION),
C   DELNA = PHASE OF RA (DASHED SOLUTION),
C   DELP = PHASE OF RB,
C   XT = VALUES OF THE THIRD LAYER THICKNESS FOR WHICH
C       CHECKS ON THE EXISTANCE OF SOLUTIONS ARE MADE,
C   X1POS = LAYER 1 OPTICAL THICKNESS (SOLID SOLUTION),
C   X1NEG = LAYER 1 OPTICAL THICKNESS (DASHED SOLUTION),
C   X2POS = LAYER 2 OPTICAL THICKNESS (SOLID SOLUTION),
C   X2NEG = LAYER 2 OPTICAL THICKNESS (DASHED SOLUTION),
C   X3 = LAYER 3 OPTICAL THICKNESS.
C
C DIMENSION X3(500),X1POS(500),X1NEG(500),X2POS(500)
C DIMENSION X2NEG(500)
C REAL*4 N0,N1,N2,N3,N4
C CHARACTER*60 HEAD1
C
C READ IN INPUT PARAMETERS. THE WAVELENGTH (MICRONS) AND INDICES
C OF REFRACTION SHOULD BE STORED IN THE FILE "INDEX.DAT" PRIOR TO
C EXECUTION.
C
C OPEN(UNIT=10,FILE="ANTIREF.DAT",ACCESS="SEQUENTIAL",
C *   FORM="FORMATTED",STATUS="NEW")
C OPEN(UNIT=11,FILE="INDEX.DAT",ACCESS="SEQUENTIAL",
C *   FORM="FORMATTED",STATUS="OLD")
C
C READ(10) N0
C READ(11,10) WVLGTH
10  FORMAT(F5.2)
C READ(11,20) N1
C READ(11,20) N2
C READ(11,20) N3
C READ(11,20) N4
20  FORMAT(F6.4)
C
C CALCULATION OF FRESNEL COEFFICIENTS AT THE VARIOUS INTERFACES.
C
C R10=(N1-N0)/(N1+N0)
C R21=(N2-N1)/(N2+N1)
C R23=(N2-N3)/(N2+N3)
C R34=(N3-N4)/(N3+N4)
C
C PI=3.1415926535

```

NWC TP 6651

```

C   CALCULATION OF THE SOLUTIONS (OR OF THE X1 AND X2 VALUES)
C   FOR EACH X3 VALUE.
C
    J=1
    XT=0.
    DO 4) I=1,501
    REMAG=(SQRT((P23+R23**2+P34*(COS(4.*PI*XT))+R34*COS(4.*PI*XT)
    **R23*R34**2)**2+R34**2*(SIN(4.*PI*XT))**2*(R23**2-1.)**2))/
    *(1.+2.*R23*R34*COS(4.*PI*XT)+P23**2+R34**2)
C
    FUNC=(R21**2+R10**2-REMAG**2*(1.+P21**2+P10**2))/(2.*R21*R10*
    *(REMAG**2-1.))
C
C   DETERMINATION OF WHETHER A SOLUTION EXISTS FOR THE PRESENT XT
C   VALUE. IF THERE IS NO SOLUTION, THEN XT IS INCREMENTED UP BY
C   0.001.
C
    IF(ABS(FUNC).GT.1.) THEN
    GO TO 30
    END IF
C
C   A SOLUTION EXISTS SO X3 IS SET EQUAL TO XT, AND THE X1 AND X2
C   VALUES ARE CALCULATED.
C
    X3(J)=XT
    X1POS(J)=(1./(4.*PI))*ACOS(FUNC)
    X1NEG(J)=-X1POS(J)
C
C   DETERMINES THE QUADRENT THAT PHASE ANGLE DELPA IS IN.
C
    DELNUM=(-R10*SIN(4.*PI*X1POS(J)))*(1.-R21**2)
    DELDEN=R21+P21**2+R10*(COS(4.*PI*X1POS(J)))+R10
    **COS(4.*PI*X1POS(J))+P21*R10**2
    IF(DELDEN.EQ.0.) GO TO 900
    DELPA=ATAN(ABS(DELNUM/DELDEN))
    IF(DELNUM.GT.0.) THEN
    IF(DELDEN.GT.0.) GO TO 2000
    END IF
    IF(DELNUM.GT.0.) THEN
    IF(DELDEN.LT.0.) GO TO 1000
    END IF
    IF(DELNUM.LT.0.) THEN
    IF(DELDEN.LT.0.) GO TO 1100
    END IF
    IF(DELNUM.LT.0.) THEN
    IF(DELDEN.GT.0.) GO TO 1200
    END IF
    IF(DELNUM.EQ.0.) THEN
    IF(DELDEN.GT.0.) GO TO 1300
    ELSE
    IF(DELDEN.LT.0.) GO TO 1400
    END IF
    900 IF(DELDEN.EQ.0.) THEN
    IF(DELNUM.GT.0.) GO TO 1500
    ELSE
    IF(DELNUM.LT.0.) GO TO 1600
    END IF
    1000 DELPA=PI-DELP
    GO TO 2000
    1100 DELPA=PI+DELP
    GO TO 2000
    1200 DELPA=2.*PI-DELP
    GO TO 2000
    1300 DELPA=0.
    GO TO 2000
    1400 DELPA=PI
    GO TO 2000
    1500 DELPA=PI/2.
    GO TO 2000
    1600 DELPA=(3.*PI)/2.

```

NWC TP 6651

```

C
C   DETERMINES THE QUADRENT THAT PHASE ANGLE DELB IS IN.
C
2000 DELNUM=(-R34*SIN(4.*PI*X3(J)))*(1.-R23**2)
    DELDEN=(R23+R23**2*R34*(COS(4.*PI*X3(J)))+R34*COS(4.*PI*
    *X3(J))+R23*R34**2)
    IF(DELDEN.EQ.0.) GO TO 2900
    DELB=ATAN(ABS(DELNUM/DELDEN))
    IF(DELNUM.GT.0.) THEN
        IF(DELDEN.GT.0.) GO TO 4000
    END IF
    IF(DELNUM.GT.0.) THEN
        IF(DELDEN.LT.0.) GO TO 3000
    END IF
    IF(DELNUM.LT.0.) THEN
        IF(DELDEN.LT.0.) GO TO 3100
    END IF
    IF(DELNUM.LT.0.) THEN
        IF(DELDEN.GT.0.) GO TO 3200
    END IF
    IF(DELNUM.EQ.0.) THEN
        IF(DELDEN.GT.0.) GO TO 3300
    ELSE
        IF(DELDEN.LT.0.) GO TO 3400
    END IF
2900 IF(DELDEN.EQ.0.) THEN
        IF(DELNUM.GT.0.) GO TO 3500
    ELSE
        IF(DELNUM.LT.0.) GO TO 3600
    END IF
3000 DELB=PI-DELB
    GO TO 4000
3100 DELB=PI+DELB
    GO TO 4000
3200 DELB=2.*PI-DELB
    GO TO 4000
3300 DELB=0.
    GO TO 4000
3400 DELB=PI
    GO TO 4000
3500 DELB=PI/2.
    GO TO 4000
3600 DELB=(3.*PI)/2.
4000 X2PCS(J)=(1./(4.*PI))*(DELPA+DELB)
C
C   DETERMINES THE QUADRENT THAT PHASE ANGLE DELNA IS IN.
C
    DELNUM=(-R10*SIN(4.*PI*X1NEG(J)))*(1.-R21**2)
    DELDEN=(R21+R21**2*R10*(COS(4.*PI*X1NEG(J)))+R10*COS(4.*PI*
    *X1NEG(J))+R21*R10**2)
    IF(DELDEN.EQ.0.) GO TO 4900
    DELNA=ATAN(ABS(DELNUM/DELDEN))
    IF(DELNUM.GT.0.) THEN
        IF(DELDEN.GT.0.) GO TO 6000
    END IF
    IF(DELNUM.GT.0.) THEN
        IF(DELDEN.LT.0.) GO TO 5000
    END IF
    IF(DELNUM.LT.0.) THEN
        IF(DELDEN.LT.0.) GO TO 5100
    END IF
    IF(DELNUM.LT.0.) THEN
        IF(DELDEN.GT.0.) GO TO 5200
    END IF
    IF(DELNUM.EQ.0.) THEN
        IF(DELDEN.GT.0.) GO TO 5300
    ELSE
        IF(DELDEN.LT.0.) GO TO 5400
    END IF

```

NWC TP 6651

```

4900 IF(GELDEN.EC.0.) THEN
      IF(DELNUP.GT.0.) GO TO 5500
      ELSE
        IF(DELNUP.LT.0.) GO TO 5600
      END IF
5000 DELNA=PI-DELNA
      GO TO 6000
5100 DELNA=PI+DELNA
      GO TO 6000
5200 DELNA=2.*PI-DELNA
      GO TO 6000
5300 DELNA=0.
      GO TO 6000
5400 DELNA=PI
      GO TO 6000
5500 DELNA=PI/2.
      GO TO 6000
5600 DELNA=(3.*PI)/2.
6000 X2NEG(J)=(1./(4.*PI))*(DELNA+DELNA)
      J=J+1
      30 XT=XT+0.001
      40 CONTINUE
C
      DO 42 I=1,J-1
      X1NEG(I)=X1NEG(I)+0.5
      X2POS(I)=X2POS(I)-0.5
      42 CONTINUE
C
C   THE OPTICAL THICKNESSES ARE WRITTEN TO THE FILE "ANTIREF.DAT".
C
      WRITE(10,43)WVLGTH,N0,N1,N2,N3,N4
43   FORMAT(1X,"WAVELENGTH = ",F5.2,"MICRONS",/,1X,"N0 = ",F6.4,/,
      *1X,"N1 = ",F6.4,/,1X,"N2 = ",F6.4,/,1X,"N3 = ",F6.4,/,1X,"N4 = ",
      *F6.4,///)
      WRITE(10,45)
45   FORMAT(3X,"X3",5X,"X1POS",3X,"X1NEG",3X,"X2POS",3X,"X2NEG",/)
      WRITE(10,50)(X3(I),X1POS(I),X1NEG(I),X2POS(I),X2NEG(I),I=1,J-1)
50   FORMAT(1X,F7.4,1X,F7.4,1X,F7.4,1X,F7.4,1X,F7.4)
C
C   PLOTTING SECTION. (USES DISPLA GRAPHICS.)
C
      CALL COMPRS
      CALL PAGE(9.5,11.0)
      CALL SWISSM
      CALL S4DCMP(90.,1,0.01,1)
      CALL AREA2D(5.,5.)
      CALL FRAME
C
C   WRITES AXIS LABELS AND THE PLOT HEADING.
C
      CALL RESET("MIXALF")
      CALL XNAME("X3 ((Wavelengths))",100)
      CALL YNAME("X1 and X2 ((Wavelengths))",100)
      CALL MIXALF("L/CGREEK")
      WRITE (HEAD1, 40) WVLGTH
60   FORMAT("Antireflectance Coating ((", F4.2, "(M)m)")
      CALL HEADIN(XREF(HEAD1), 100, 1.5, 1)

```

NWC TP 6651

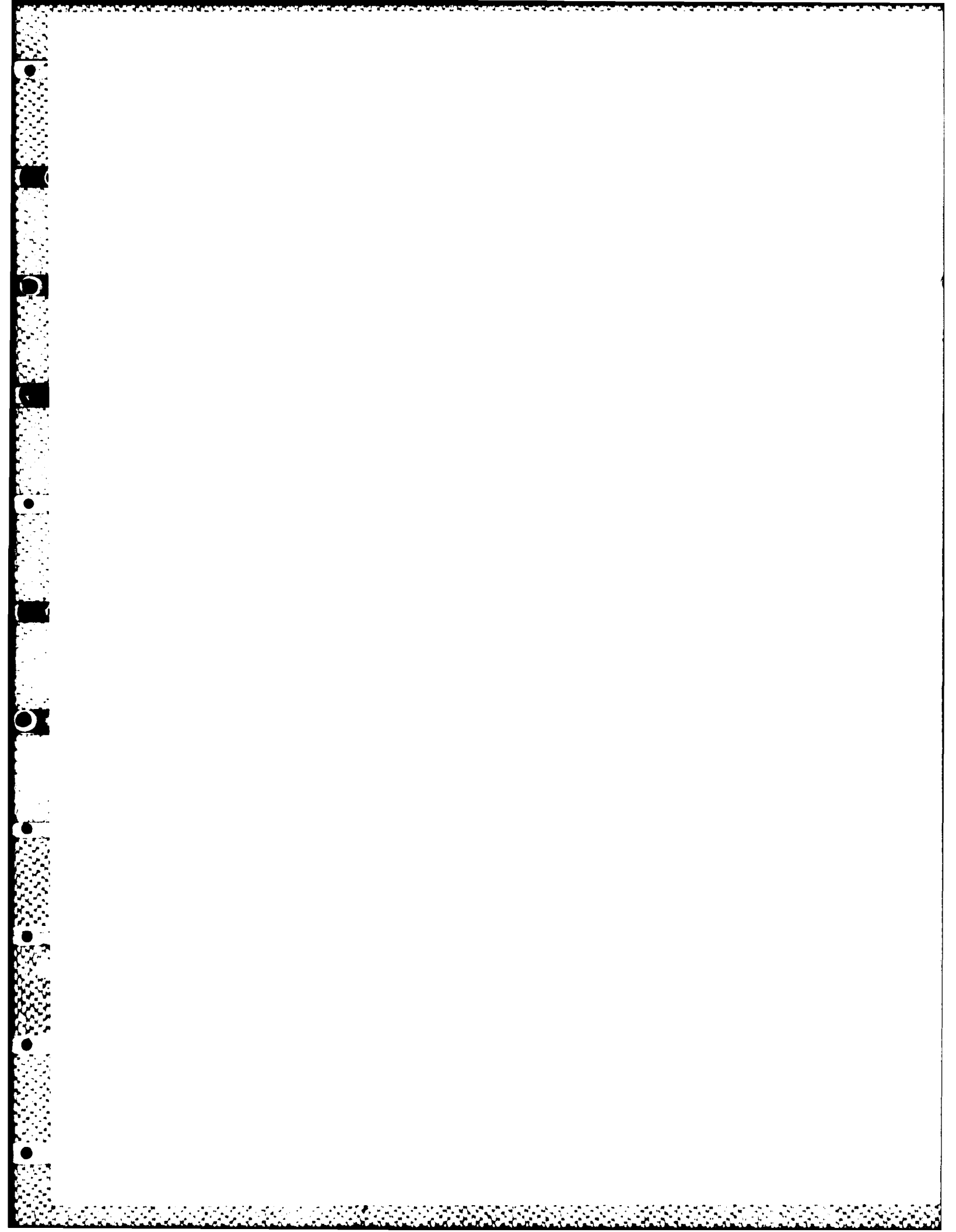
C  
C  
C  
C

PLOTS Y1 AND X2 VS. X3. A SPLINE CURVE FITTING ROUTINE IS USED  
FOR FITTING THE DATA.

```
CALL GRAF(0.,0.1,0.5,0.,0.1,0.5)
CALL RASPLN(0)
CALL T-RERV(0.03)
CALL BL-CURV(0.02,0.02)
CALL CURVE(X3,X1PDS,J-1,0)
CALL CURVE(X3,X2PDS,J-1,0)
CALL DASH
CALL CURVE(X3,X1NEG,J-1,0)
CALL CURVE(X3,X2NEG,J-1,0)
CALL RESET("DASH")
CALL ENDFL(0)
CALL DONEPL
END
```

## INITIAL DISTRIBUTION

- 2 Naval Air Systems Command (AIR-723)
- 2 Naval Sea Systems Command (SEA-09B312)
- 1 Commander in Chief, U.S. Pacific Fleet (Code 325)
- 1 Commander, Third Fleet, Pearl Harbor
- 1 Commander, Seventh Fleet, San Francisco
- 2 Naval Academy, Annapolis (Director of Research)
- 3 Naval Ship Weapon Systems Engineering Station, Port Hueneme
  - Code 5711, Repository (2)
  - Code 5712 (1)
- 1 Naval War College, Newport
- 1 Army Materials and Mechanics Research Center, Watertown (T. V. Hynes)
- 1 Air Force Intelligence Service, Bolling Air Force Base (AFIS/INTAW, Maj. R. Lecklider)
- 12 Defense Technical Information Center
  - 1 Battelle Pacific Northwest Laboratories, Richland, WA (W. T. Pawlewicz)
  - 1 Burleigh Northwest Optical, Inc., Fishers, NY (D. R. Sigler)
  - 1 Coherent Medical Group, Palo Alto, CA (E. A. Nevis)
  - 1 Martin Marietta Aerospace, Albuquerque, NM (T. Raj)
  - 1 Northrop Research and Technology Center, Palos Verdes Peninsula, CA (S. J. Holmes)
  - 1 University of Missouri, Columbia, MO (R. M. O'Connell)



END

FILMED

3 - 86

DTIC